

Electronic Supplementary Information(ESI†)

Benzothiazole conjugated hemicyanine dye as ratiometric NIR fluorescent probe for detection and imaging of peroxynitrite in living cells

Uday Narayan Guria,^a Ankita Gangopadhyay,^a Syed Samim Ali,^a Kalipada Maiti,^a Sandip Kumar Samanta,^a Srimanta Manna,^a Asim Kumar Ghosh,^b Md. Raihan Uddin,^c Sukhendu Mandal^c and Ajit Kumar Mahapatra^{*a}

^aDepartment of Chemistry, Indian Institute of Engineering Science and Technology, Shibpur, Howrah-711103, West Bengal, India, Email: akmahapatra@rediffmail.com, Fax: +913326684564

^bbhabha atomic research centre, Trombay. Mumbai-400085, India

^cDepartment of Microbiology, University of Calcutta, Kolkata- 700019.

Contents

1. ¹H NMR spectrum of Compound 2 DMSO-d₆.
2. ESI-MS mass spectrum of Compound 3
3. ¹H NMR of compound Compound 3 in DMSO-d₆
4. ESI-MS mass spectrum of BPVI
5. ¹H NMR of BPVI in CDCl₃
6. ¹³C NMR of BPVI
7. Comparative visible and Fluorescence colour change.
8. Determination of detection limit.
9. Competitive fluorescence bar diagram of BPVI.
10. HR-MS (partial) of sample withdrawn from assay system.
11. Fluorescence signal of only aldehyde (3).
12. Kinetic Study of BPVI.
13. Optimized molecular structures and molecular orbital.
14. DFT calculation table.
15. MTT assay.

16. The summary table of lately OONO⁻ probe.

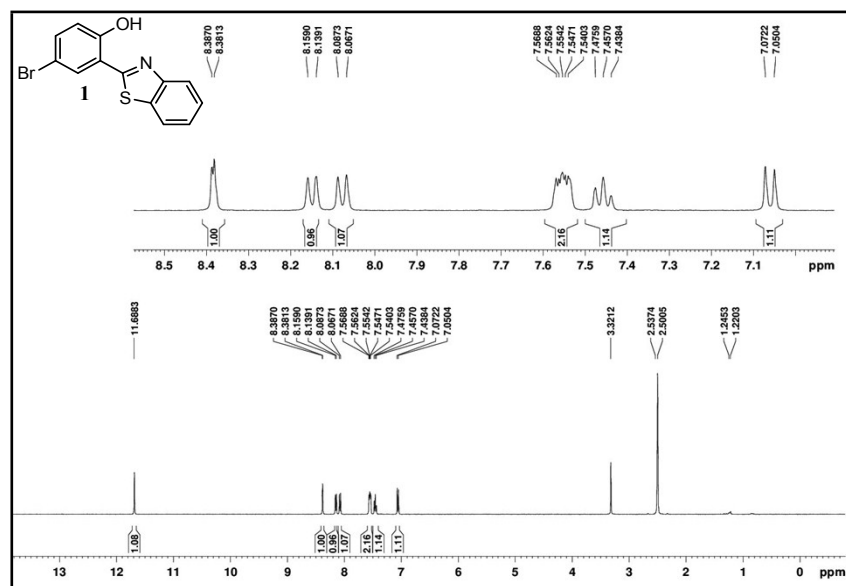


Figure S1. ¹H NMR spectrum of Compound 2 DMSO-d₆.

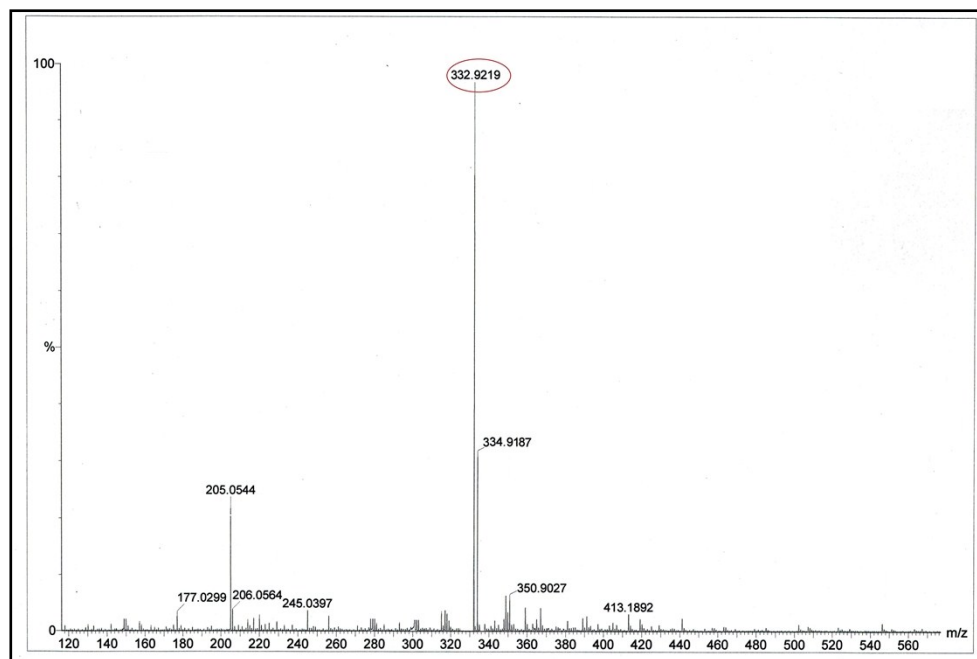


Figure S2. ESI-MS mass spectrum of Compound 3

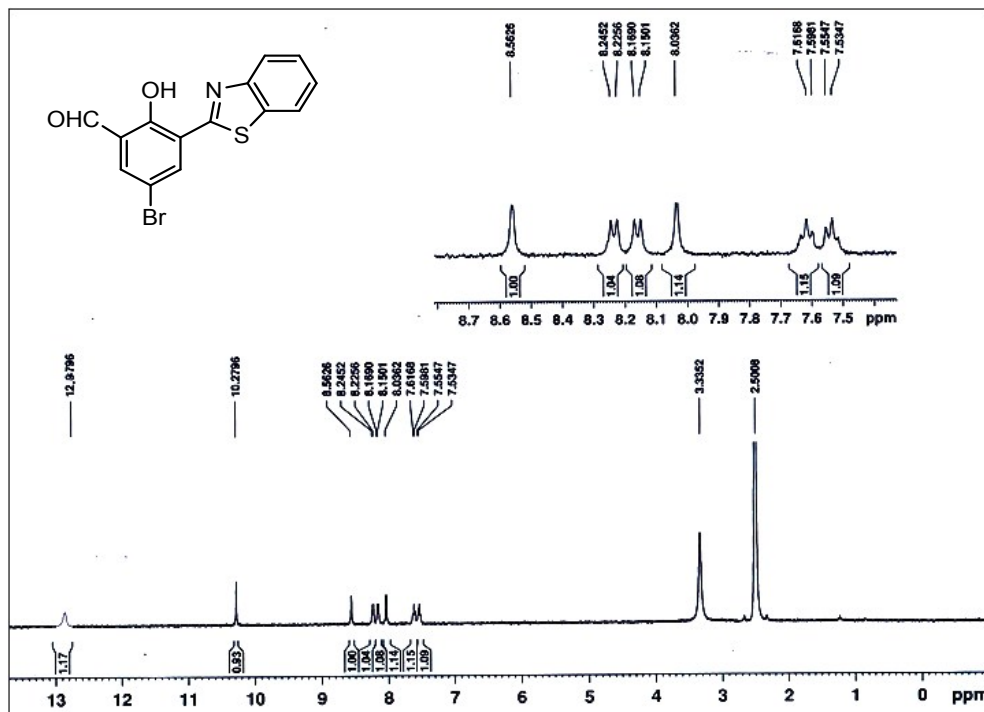


Figure S3. ¹H NMR of compound Compound 3 in DMSO-d₆

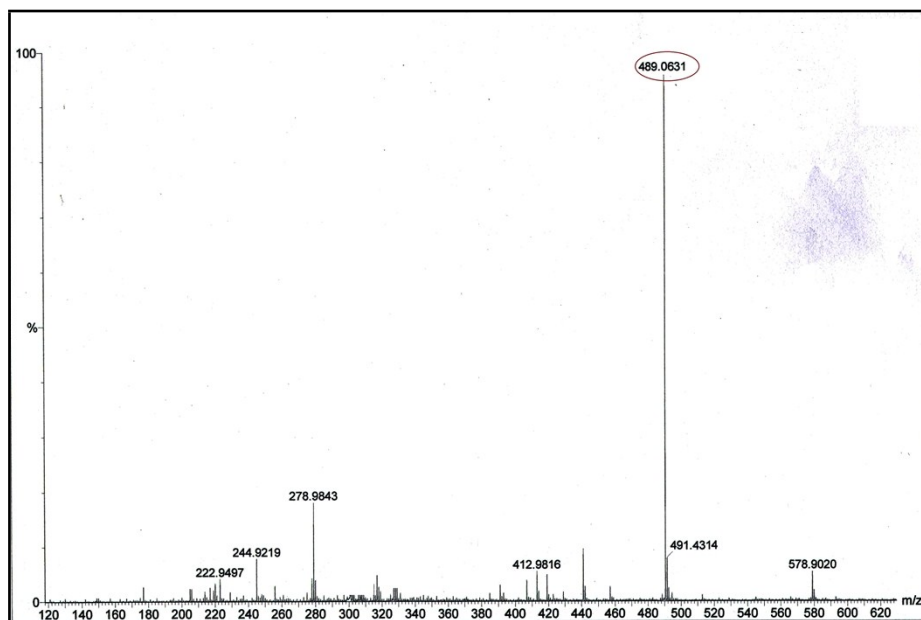


Figure S4. ESI-MS mass spectrum of BPVI

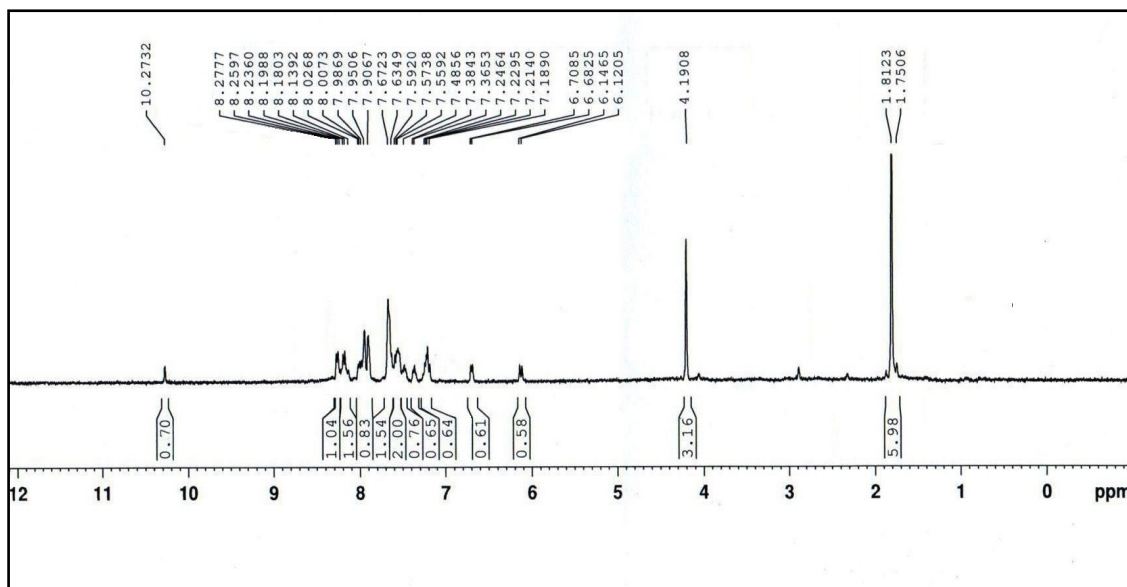


Figure S5. ^1H NMR of BPVI in DMSO- d_6 .

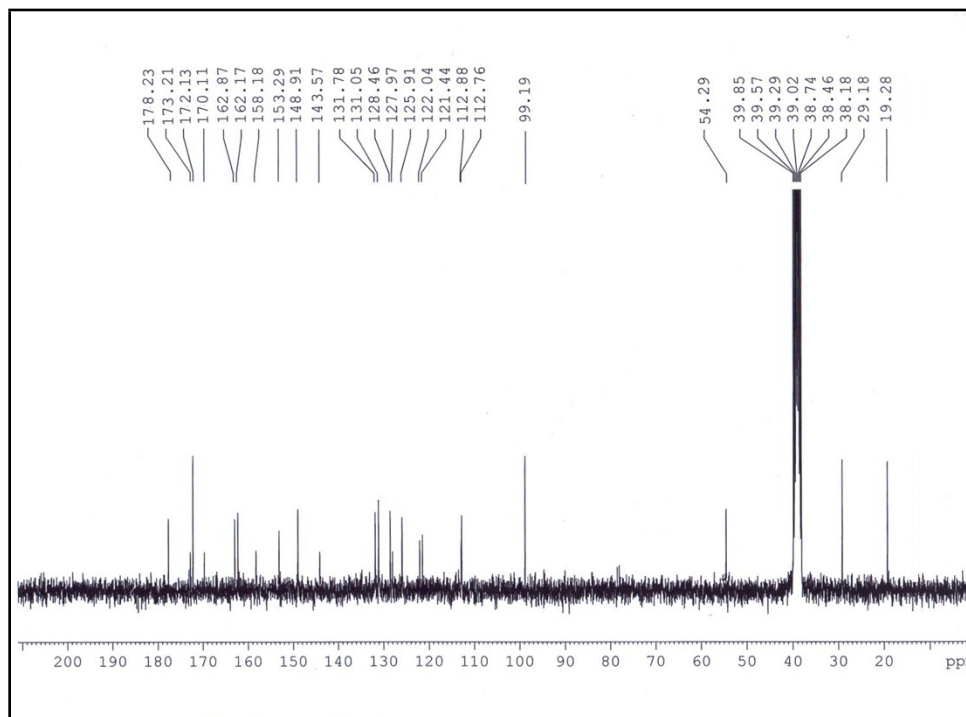


Figure S6. ^{13}C NMR of BPVI

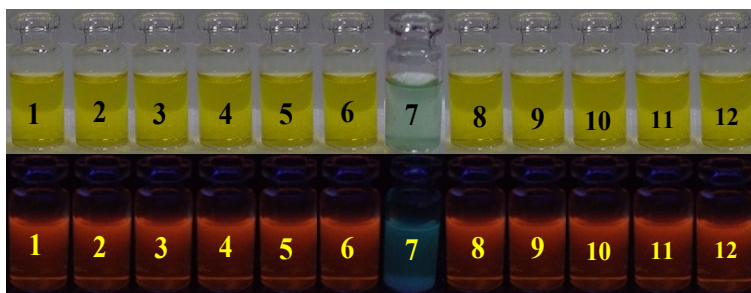


Figure S7. The visible color (top) and fluorescence changes (bottom) of receptor **BPVI** in aq. AcCN (1.0 μM , 20 mM HEPES buffer PH 7.4, AcCN-H₂O; 1:2; v/v) upon addition of ONOO⁻ (20 μM) and various analytes (50 μM). (1) Probe, (2) ROO[•], (3) NO, (4) t-BuOOH, (5) OCl⁻, (6) H₂O₂, (7) ONOO⁻, (8) Hcy, (9) Cys, (10) NaSH, (11) GSH, (12) NO₂⁻.

Calculation of Detection limit:

The detection limit (DL) of **BPVI** for ONOO⁻ were determined from the following equation:

$$\text{DL} = K * \text{Sb1}/S$$

Where K = 2 or 3 (we take 2 in this case); Sb1 is the standard deviation of the blank solution; S is the slope of the calibration curve.

From graph S = 372737.80, Sb1=0.00703, DL= 37 nM

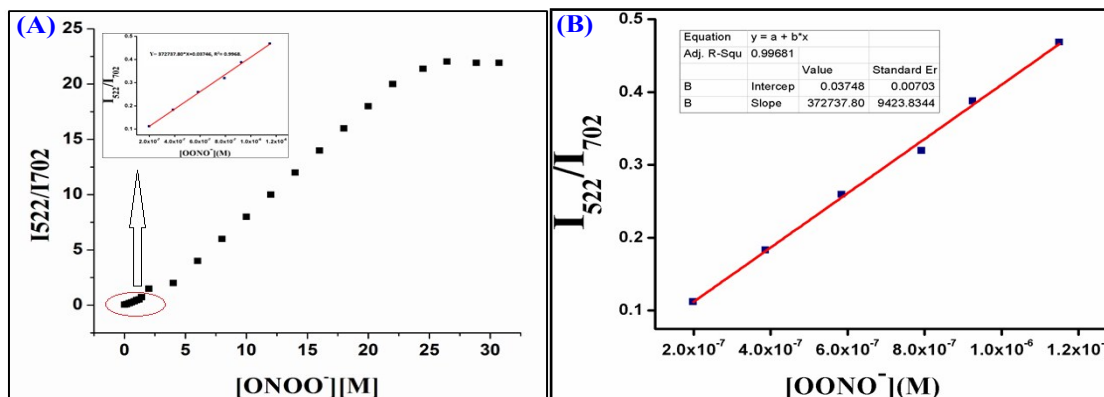


Figure S8. (A) Dependence between the fluorescence intensity at I_{522}/I_{702} nm nm and the concentration of peroxyntirite, The inset showed the linear dependence of intensity with

concentration. **(B)** Calibration curve for Fluorescence titration of **BPVI** at I_{522}/I_{702} nm (Ex@451nm) with OONO^- .

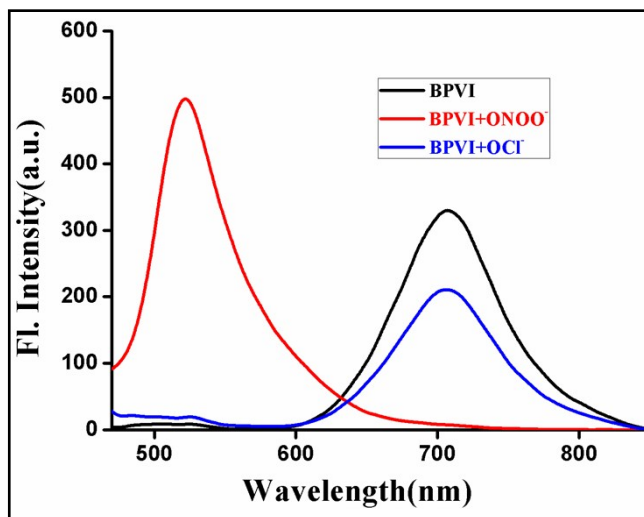


Figure S9. Spectral response of the probe **BPVI** ($1.0 \mu\text{M}$) with OONO^- and OCl^- (200 equiv.).

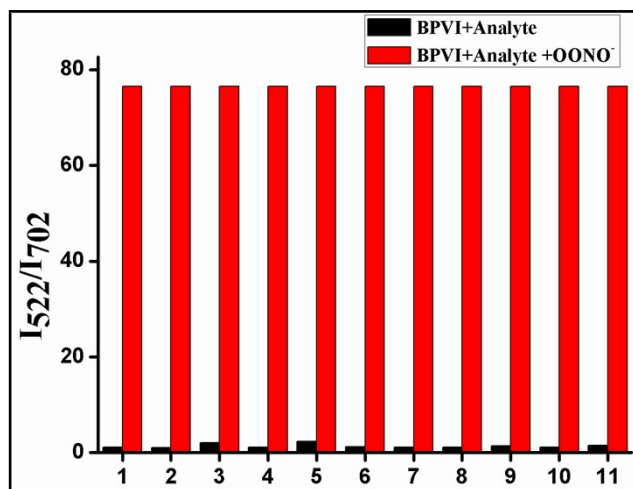


Figure S10. Change in fluorescence spectra of **BPVI** (at I_{522}/I_{702} nm) ($c= 1 \times 10^{-5}$ M) to 100 eqv. of other analytes [Small black bars] and to the mixture of 100 eqv. of other analytes 1, BPVI; 2,

NO_3^- ; 3, NO ; 4, NO_2^- ; 5, OCl^- ; 6, H_2O_2 ; 7, ONOO^- ; 8, $\cdot\text{O}_2^-$; 9, $\cdot\text{OH}$; 10, $\text{ROO}\cdot$; 11, GSH ;] 10 eqv. addition of OONO^- [Big red bars].

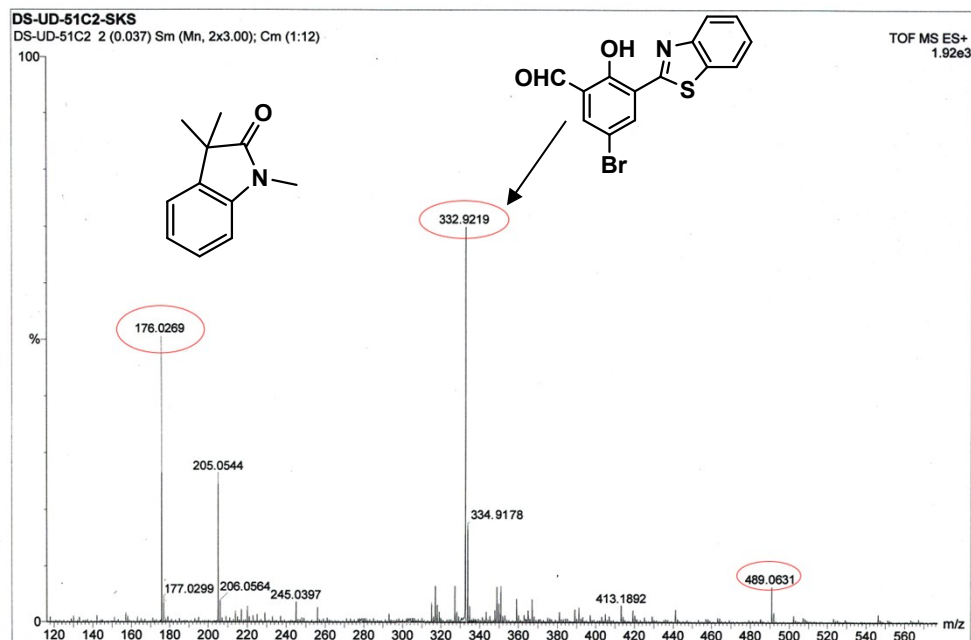


Figure S11. HR-MS (partial) of sample withdrawn from assay system.

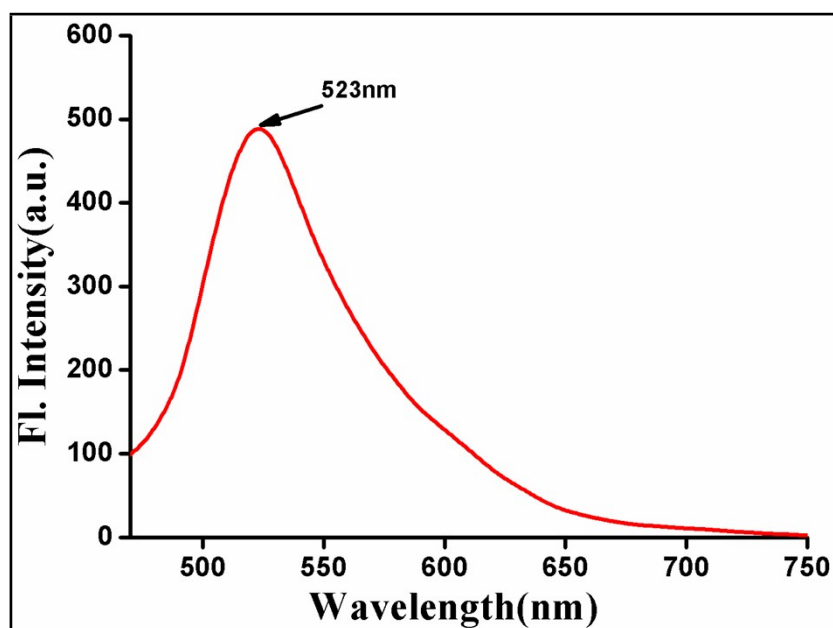


Figure S12. Fluorescence signal of only aldehyde (**3**) excited at 451nm.

Kinetic Study:

The solution phase chemodosimetric reactions of **BPVI** in AcCN were followed by measuring the fluorescence spectra after mixing **BPVI** and ONOO^- in a cubic 4-sided quartz cell of 3 ml. The reaction was carried out at 35°C under the excess amount of ONOO^- (25-100 eqv.) (Initial concentration $[\text{BPVI}] \ll [\text{ONOO}^-]$) and the reaction was expected to reach 100% conversion. Separate solutions of different concentrations of **BPVI** and ONOO^- in AcCN were prepared and mixed to investigate the kinetics. The excitation wavelength was 500 nm and in all cases the concentration was low enough to maintain a UV absorption that was < 0.1 . The rate of the reaction was determined by fitting the fluorescence intensities of the samples to the Pseudo-First Order Equation (1):

$$\ln(F_{\max} - F_t)/F_{\max} = -k/t \dots\dots\dots(1)$$

Where $F(t)$ and $F(\max)$ are the fluorescence intensities at the monitoring wavelengths at times t and the maxima values which are the last fluorescence intensities when **BPVI** reached the conversion of 100%. The k is the apparent rate constant. Figure S13 is the pseudo first order plot of **BPVI** with 100 equiv. of ONOO^- . The negative slope of the plot shows the apparent rate constant = 0.00836 S^{-1} .

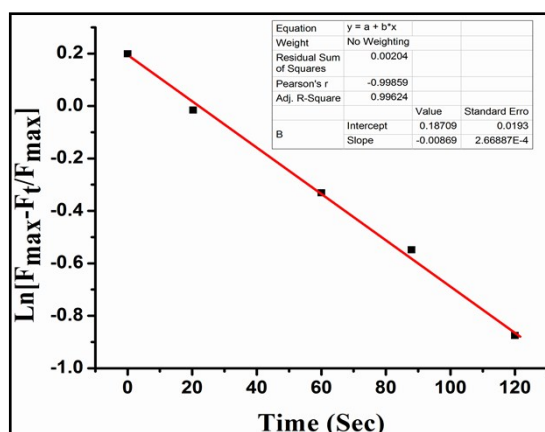


Figure S13. (a) Pseudo first-order kinetic plot of reaction of **BPVI** (1.0µM) with ONOO^- (30 equiv.) in AcCN. Slope = 0.00836 S^{-1} .

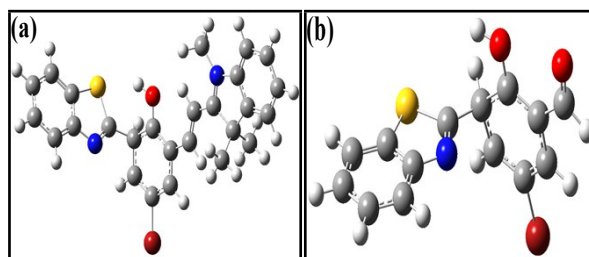


Figure S14. Optimized molecular structures and molecular orbitals of **BPVI** and **Compound 3**.

Table S1. Selected electronic excitation energies (eV), oscillator strengths (f), main configurations, and CI Coefficients of all the complexes. The data were calculated by TDDFT//B3LYP/6-31+G (d,p) based on the optimized ground state geometries

Molecules	Excitation Energy ^a	f^b	Composition ^c	(composition) %
BPVI	1.987 eV 619.95 nm	0.0905	H \rightarrow L	87.7
	2.6806 eV 462.53 nm	0.0344	H \rightarrow L+1	86.1
	2.7738 eV 446.98 nm	0.0309	H \rightarrow L+2	53.4
	2.9844 eV 415.45 nm	0.07127	H-1 \rightarrow L+3	68.2
Compound 3	3.1163 eV 398 nm	0.00914	H \rightarrow L+1	51.02
	2.7815 eV 445.95 nm	0.0221	H \rightarrow L	87.23

Computational details:

Geometries have been optimized using the B3LYP/6-31+G (d,p) level of theory. The geometries are verified as proper minima by frequency calculations. Time-dependent density functional theory calculation has also been performed at the same level of theory. All calculations have been carried out using Gaussian 09 program.

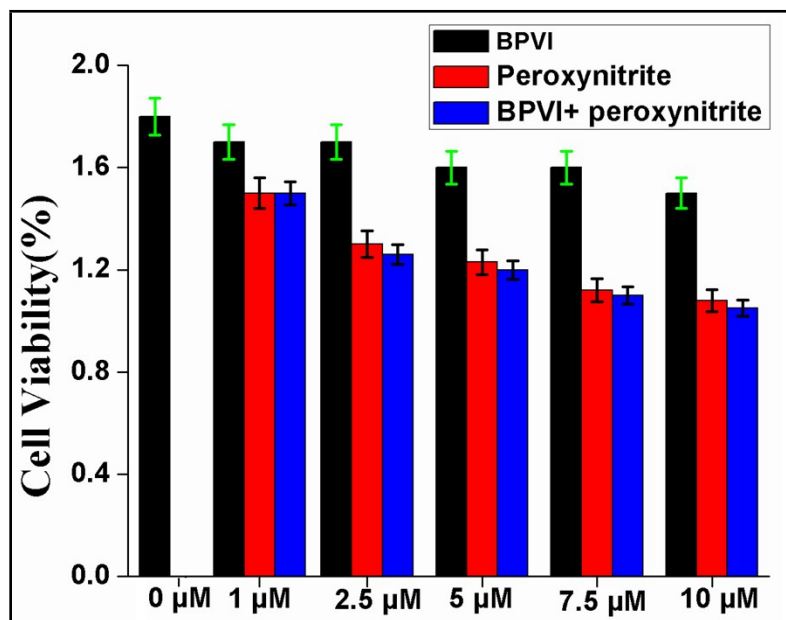


Figure S15. MTT assay to determine the cytotoxic effect of **BPVI** and ONOO^- -complex on adenocarcinomic human alveolar basal epithelial cells including error bars [error amount, 4% (for **BPVI**, ONOO^- and 3% for **BPVI+ ONOO}^-); Y error bar for both $[\pm]$ deviations].**

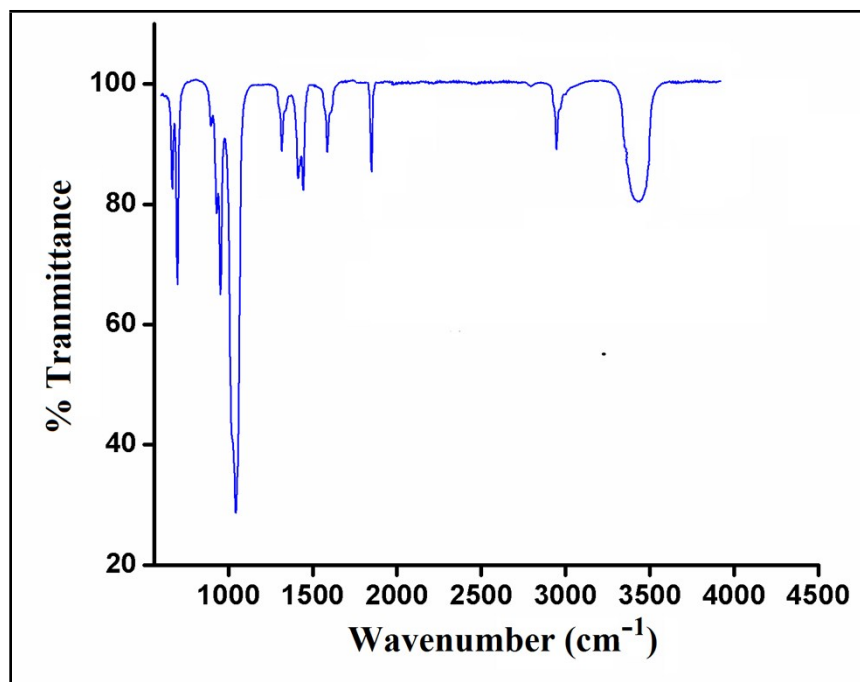
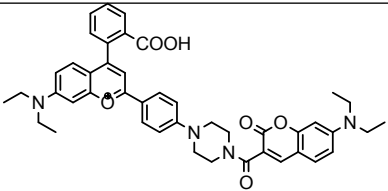
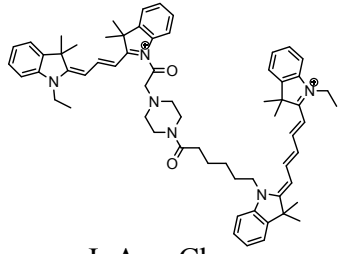
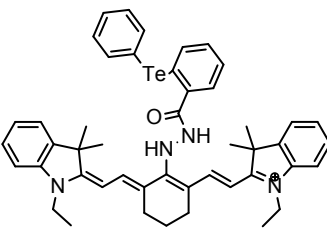
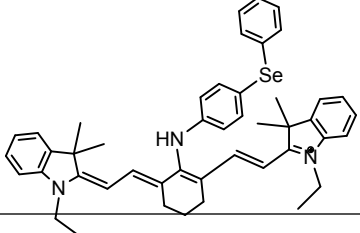
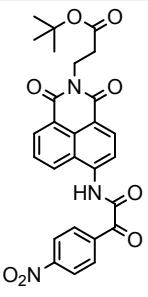
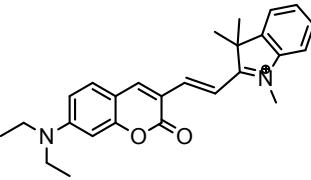
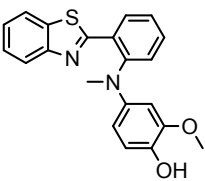
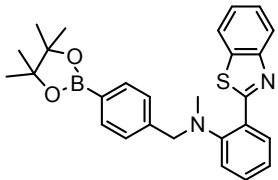
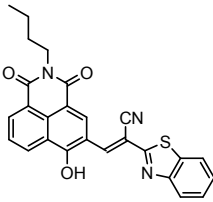


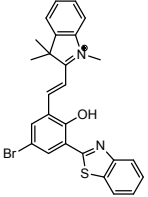
Figure S16. IR spectra of BPVI.

The compared table of lately OONO⁻ probe:

Table S2 Summary of lately reported fluorescent probes for OONO⁻.

Probe	Sensing Mechanism	$\lambda_{ex}/\lambda_{em}$	Stokes Shift	LOD
 <p>J. Am. Chem. Soc. 2017, 139, 285-292</p>	FRET	420nm 473nm/651nm	N.A	11.30nM
 <p>J. Am. Chem. Soc.2016,138,10778-10781</p>	FRET	530nm 560nm/660nm	30nm 20nm	0.65nM
 <p>J. Am. Chem. Soc. 2013,135, 7674-7680.</p>	PET	793nm 820nm	27nm	0.917 μ M
	PET	758nm 775nm	17nm	N.A

J. Am. Chem. Soc. 2011, 133, 11030-11033.				
 Chem. Sci. 2017, 8, 4006-4011	ICT	430nm 560nm	130nm	25nM
 Biosens. Bioelectrons. 2015, 64, 285-291.	ICT	475nm 515nm/635nm	N.A	49.7nM
 J. Am. Chem. Soc. 2015, 137. 12296-12303	ESIPT	375nm 470nm	95nm	5.0nM
 Chem.Comm. 2016, 52, 12350-12352.	ESIPT	400nm 461nm	61nm	N.A
 RSC Adv. 2018, 8, 1826-1832.	ESIPT/ ICT	405nm 518nm	103nm	37nM

 <p>This Work.</p>	ESIPT/ ICT	451nm 522nm/702nm	71nm/ 251nm	37nM
---	---------------	----------------------	----------------	------